

Analytical solution for doubly-periodic harmonic problems with circular inhomogeneities and superconducting or membrane-type interfaces

Anna Y. Zemlyanova^a, Yuri A. Godin^b, Sofia G. Mogilevskaya^{c*}

Wednesday 8th December, 2021

^{a)}*Department of Mathematics, Kansas State University, 138 Cardwell Hall, Manhattan, Kansas, 66506, USA*

^{b)}*Department of Mathematics and Statistics, University of North Carolina at Charlotte, Charlotte, NC 28223, USA*

^{c)}*Department of Civil, Environmental, and Geo- Engineering, University of Minnesota, 500 Pillsbury Drive S.E., Minneapolis, MN, 55455, USA*

Abstract

A novel analytical solution for two-dimensional harmonic problems involving doubly-periodic arrays of circular inhomogeneities with superconducting or membrane type interfaces is derived. The complex potential inside each inhomogeneity is sought in the form of power series, while its counterpart inside the matrix is represented by the series in terms of Weierstrass ζ -function and its derivatives. Compliance with the interface conditions results in an infinite system of linear algebraic equations for unknown series coefficients. A rigorous theoretical study of the system properties is performed. The solution is used for evaluating the local fields and overall properties of composites. For the case of square and hexagonal unit cells, accurate formulas for the effective properties

*Corresponding author. E-mail address: mogil003@umn.edu (S.G. Mogilevskaya)

are provided. Numerical examples are presented and comparison with the results reported in the literature is performed.

Keywords: Composite materials; Doubly-periodic harmonic problems; Analytical solution; Local fields; Overall properties.

1 Introduction

In this paper, we derive a novel analytical solution for two-dimensional harmonic problems involving doubly-periodic arrays of circular inhomogeneities with imperfect interfaces of a specific type. Depending on the area of application, this type is referred to as superconducting/ highly conducting interface (e.g. in heat or electrical conduction, dielectrics, etc.) or membrane/Gurtin-Murdoch interface (in antiplane elasticity).

In the context of thermal conduction, the conditions across the superconducting interface are those of continuity of the temperature and jump in the normal component of the heat flux; the latter is proportional to the surface Laplacian of the temperature at the interface. Such conditions could be used for modeling problems involving coated fibers with thin and highly conducting interphases, see [1]. The studies of superconducting interfaces started in the late 1990s and the review of the early literature on the topic can be found in [2]. Those early studies produced various estimates of overall properties of isotropic composites with superconducting interfaces, rigorous variational bounds, and a few analytical approaches for solving periodic problems, mostly using Rayleigh's approach modified to account for the effects of spherical interfaces, see [3].

Since then, significant progress has been made both in theoretical and numerical modeling of isotropic and anisotropic composites with superconducting interfaces. The relevant developments included various modifications of classical homogenization schemes (dilute, Mori-Tanaka, self-consistent, and generalized self-consistent) to incorporate the effects due to superconducting interfaces (e.g., [4, 5, 6, 7, 8], and the references therein), derivations of more accurate bounds [9], semi-analytical ([5, 10]), and numerical solutions (e.g., [11, 12, 13], and the references therein).

In the context of elasticity, the corresponding conditions across the interface are those of continuity of the displacements and jump in the normal component of tractions; the latter is proportional to the surface Laplacian of the displacements at the interface. Such conditions could be used to model problems involving coated fibers with thin and stiff interphases of the so-called membrane-type, see [14], and that is the reason for the use of the notion of "membrane-type" interface. In recent two decades, interest in materials with membrane-type interfaces increased significantly due to the need to model nanomaterials that possess improved mechanical, thermal, electrical, and other properties. One of the most popular tools for modeling nanomaterials is the Gurtin-Murdoch theory ([15, 16]), which endows an interface (referred in the theory as a material surface) with its own energetic structure characterized by

surface elasticity parameters and surface tension. It was later demonstrated in e.g., [17, 18, 19] that the Gurtin-Murdoch conditions across the material surface are identical to those for the membrane-type interface when the surface tension is neglected. Moreover, even more recently, it was clarified (see [20, 21]) that, in an antiplane elasticity setting, surface tension must be excluded from the model for consistency of the latter. With that clarification, the interface conditions of the Gurtin-Murdoch model are, indeed, identical to those for the membrane-type interface. Antiplane problems with the clarified Gurtin-Murdoch interface conditions were solved numerically in [22].

Doubly-periodic problems play an important role in homogenization procedures and during the last decade several methods were proposed to model such problems for composites with superconducting or membrane-type interfaces. As the present paper deals with two-dimensional problems, here we only perform review of relevant literature. The thermal conduction problems involving doubly-periodic materials with square or rectangular unit cells that contain square, hexagonal, and random arrays of inhomogeneities were considered in [10] both in two- and three dimensions. The latter paper mostly focused on the determination of the effective properties of composites with overall isotropy. The authors split the fields into the uniform and periodic perturbation parts and used discrete Fourier transform to solve the balance equation for the perturbation parts. As the iterative numerical procedure in the transform space was employed, the solution cannot be regarded as fully analytical. Castro et al [23] considered the problem that involves square unit cell and reformulated the problem in terms of a complex potential with the doubly-periodic real part. They used Taylor series expansions inside the inhomogeneities to solve for the unknown potentials using the method of functional equation, see [24] and the references therein. The same technique was used in [25], where the thermal conductivities of the phases were assumed to be temperature-dependent. In [23, 25], the results for the local fields and overall anisotropic properties were presented for the example involving a square unit cell with four inhomogeneities. The approach of those papers is analytical but it is not clear if it could be extended to the cases of unit cells of different shapes. Kuo [26] studied more general doubly-periodic problems of piezoelectric and piezomagnetic composites with membrane-type interfaces under longitudinal shear. The potentials for the inhomogeneities and the matrix were sought in the forms of a series of trigonometric functions. Modified Rayleigh method was used to find the unknown coefficients and the results for the hexagonal arrays of inhomogeneities were presented. Gao et al. [5] studied the doubly-periodic thermal conduction problem with square and hexagonal unit cells and various interface conditions, including those of highly conducting interface. These authors used the locally-exact homogenization theory in which the fields are split into the average and local (fluctuating) parts and the governing differential equations are reformulated in terms of those fields. The equations are solved using the series expansions in terms of trigonometric functions, enforcing the interface conditions in the weak form, and using the Trefftz method.

It can be concluded from the above analysis that, despite significant progress in modeling doubly-periodic problems with superconducting or membrane-type inter-

faces, there still exists room for new analytical tools to tackle those problems. One such tool was devised in [27] for problems with perfectly bonded inhomogeneities. It is based on the use of quasi-periodic potential constructed using the Weierstrass ζ -function and its derivatives. The attractive feature of this approach is the possibility to obtain highly accurate estimates of the overall properties of composites with unit cells of some regular shapes. Another conclusion from the analysis of relevant literature is that there still exists a lack of reliable benchmark solutions as, for the most part, each of the papers presented its own set of numerical examples.

Thus, the present work has three principal goals. The first goal is to derive exact series solutions for the doubly-periodic problems with the parallelogram unit cells and perform a rigorous theoretical analysis of the solutions' properties, including uniqueness, existence, and convergence. The second goal is to obtain accurate estimates of the overall properties of composites with the square and hexagonal unit cells. The third goal is to systematically analyze existing numerical results for the local fields and effective properties of doubly-periodic composites with the unit cells of various shapes, compare those results with the derived analytical solutions in order to establish rigorous benchmark examples that could be used by future investigators.

The paper is structured as follows. In Section 2 we formulate the problem under study, present the governing equations and interface conditions, and reformulate them in terms of complex potentials. In Section 3, we provide analytical series expansions for the potentials and reduce the problem to an infinite system of linear algebraic equations for the unknown coefficients involved in the series; a rigorous theoretical study of the properties of the obtained system is described in Appendix. In Section 4, we discuss the procedures for evaluating the local fields and the overall elastic properties of composites under study. In Section 5, we present formulas for the overall properties of composites with the square and hexagonal unit cells. Section 6 contains several numerical examples and comparisons with the results of previous studies. Finally, concluding remarks are presented in Section 7.

2 Problem formulation

Consider a two-dimensional harmonic problem (e.g. steady-state thermal or electrical conduction, antiplane elasticity, etc.) involving a composite system consisting of matrix and identical circular inhomogeneities of radii a that form a doubly-periodic lattice (Fig. 1) generated by the periods $2\omega_1$ and $2\omega_2$. Assume that each phase of that system is homogeneous and isotropic, so its property is characterized by one parameter whose meaning depends on the phenomena under study. For illustration purposes, here we describe the problem in the context of antiplane elasticity where the parameters are the longitudinal shear moduli of the matrix and the inhomogeneities denoted as μ and μ_1 correspondingly. Assume that the system is subjected to the shear stress at infinity with the components σ_{13}^∞ and σ_{23}^∞ .

The displacement vector and the stress tensor for each phase of the system can

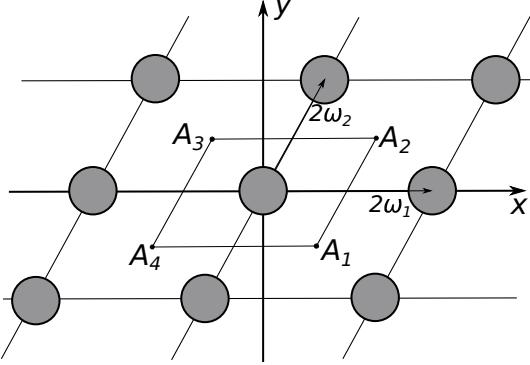


Figure 1: Composite system with doubly-periodic array of inhomogeneities.

be represented in the following forms:

$$\mathbf{u} = \begin{bmatrix} 0 \\ 0 \\ u_3 \end{bmatrix}, \quad \boldsymbol{\sigma} = \begin{bmatrix} 0 & 0 & \sigma_{13} \\ 0 & 0 & \sigma_{23} \\ \sigma_{13} & \sigma_{23} & 0 \end{bmatrix}, \quad (2.1)$$

where all non-zero components are independent of x_3 and given by the following functions of x_1, x_2 :

$$u_3 = u_3(x_1, x_2), \quad \sigma_{13} = \sigma_{13}(x_1, x_2), \quad \sigma_{23} = \sigma_{23}(x_1, x_2). \quad (2.2)$$

As the displacement $u_3(x_1, x_2)$ satisfies the Laplace equation

$$\nabla^2 u_3 = \frac{\partial^2 u_3}{\partial x_1^2} + \frac{\partial^2 u_3}{\partial x_2^2} = 0, \quad (2.3)$$

it is possible, e.g., [28], to express the non-zero components of the stress tensor and the displacements vector in each phase via the corresponding analytic function (complex potential) as

$$u_3 = \text{Im } f(z), \quad \sigma_{23} + i\sigma_{13} = \mu f'(z), \quad (2.4)$$

$$u_3^1 = \text{Im } f_1(z), \quad \sigma_{23}^1 + i\sigma_{13}^1 = \mu_1 f_1'(z), \quad (2.5)$$

where $z = x_1 + ix_2$, and the expressions with the index “1” are related to the inhomogeneity, while the expressions without that index are related to the matrix.

The complex potential for the matrix at infinity has the form:

$$f(z) = \frac{\sigma_{23}^\infty + i\sigma_{13}^\infty}{\mu} z + O(1). \quad (2.6)$$

The conditions across each matrix/inhomogeneity boundary (interface) are assumed to be of membrane-type and, in context of antiplane elasticity, they coincide with the conditions for the Gurtin-Murdoch model that endows the interface with its own surface stress σ^S and shear modulus μ_0 . Those conditions include the

requirements of continuity of displacements and the following jump in the normal components of tractions (see [20]):

$$\mathbf{n} \cdot [\boldsymbol{\sigma}] = \partial \boldsymbol{\sigma}^S / \partial s = \mu_0 \partial^2 u_3 / \partial s^2, \quad (2.7)$$

where $[\boldsymbol{\sigma}] = \boldsymbol{\sigma}^1 - \boldsymbol{\sigma}$ denotes the jump of tractions across the boundary of some inhomogeneity, \mathbf{n} is the outward unit normal to that boundary, and s is its arc length parameter.

Introducing the polar coordinates system centered at the origin and taking into account Eqs. (2.7) and (2.1), one can rewrite the interface conditions as

$$u_3^1(t) = u_3(t), \quad (2.8)$$

$$\sigma_{r3}^1(t) - \sigma_{r3}(t) = \frac{\mu_0}{a^2} u_{3,\theta\theta}^1(t), \quad (2.9)$$

where $f_{,\theta\theta} = \partial^2 f / \partial \theta^2$ and t is the complex variable that indicates the points located at the boundary $|t| = a$ of the selected inhomogeneity.

Conditions (2.8), (2.9) can be used to accurately approximate a thin and stiff coating layer of the so-called *membrane-type*, if μ_1 and μ are roughly of the same order of magnitude, but the thickness h_l of the layer and its shear modulus μ_c behave as

$$\frac{2\mu_c}{\mu_1 + \mu} \frac{h_l}{H} \sim \Theta(1), \quad (2.10)$$

when $\mu_c/\mu \rightarrow \infty$ and $h_l/H \rightarrow 0$, in which H is some characteristic length-scale of the problem. The big- Θ symbol means an asymptotically tight bound.

In such case, the parameter μ_0 must be related to that for the layer as

$$\mu_0 = \mu_c h_l. \quad (2.11)$$

Using Eqs. (2.4), (2.6), one can rescale conditions (2.8), (2.9) as

$$\operatorname{Im} f_1(at) = \operatorname{Im} f(at), \quad |t| = 1, \quad (2.12)$$

$$\mu_1 \operatorname{Im} (f_{1,t}(at) e^{i\theta}) - \mu \operatorname{Im} (f_{,t}(at) e^{i\theta}) = \frac{\mu_0}{a} \frac{\partial^2}{\partial \theta^2} (\operatorname{Im} f_1(at)), \quad |t| = 1. \quad (2.13)$$

We emphasize again that the equations and interface conditions described in this section remain valid for other phenomena governed by the Laplace equation if the meanings of the fields involved are properly adjusted. For example, in the context of steady-state thermal conductivity, the temperature and its gradient should be used instead of the displacement and stresses involved in the antiplane problem.

3 Series representations of complex potentials

Due to the symmetry of the problem, we will look for the solutions that are odd with respect to the chosen polar coordinate system, i.e.

$$u_3(z) = -u_3(-z), \quad u_3^1(z) = -u_3^1(-z).$$

Correspondingly, the complex potentials in the matrix and inside the inhomogeneity can be represented by the series:

$$f_1(az) = a \sum_{n=0}^{\infty} (A_n + iB_n) z^{2n+1}, \quad |z| \leq 1, \quad (3.1)$$

$$f(az) = \Gamma a z + a \sum_{n=0}^{\infty} \frac{(C_n + iD_n)}{(2n)!} \zeta^{(2n)}(z), \quad z \in \mathcal{D}, \quad (3.2)$$

where \mathcal{D} is the domain representing the exterior of the doubly-periodic lattice of identical circles of unit radii with periods $2\omega_1/a$ and $2\omega_2/a$ and $\zeta^{(2n)}(z)$ denotes the derivative of the order $2n$ of the Weierstrass ζ -function:

$$\zeta(z) = \frac{1}{z} + \sum_{m,n} ' \left[\frac{1}{z - P_{m,n}} + \frac{1}{P_{m,n}} + \frac{z}{P_{m,n}^2} \right], \quad (3.3)$$

in which the sum is extended over all integer pairs of m, n , except for $m = n = 0$, and $P_{m,n} = 2m\omega_1/a + 2n\omega_2/a$. The properties of the function $\zeta(z)$ are described in the detail in [29]. In particular, the function $\zeta(z)$ has the quasiperiodicity property:

$$\zeta(z + 2\omega_1/a) = \zeta(z) + 2\eta_1, \quad \eta_1 = \zeta(\omega_1/a), \quad (3.4)$$

$$\zeta(z + 2\omega_2/a) = \zeta(z) + 2\eta_2, \quad \eta_2 = \zeta(\omega_2/a).$$

The derivatives $\zeta^{(2n)}(z)$ can be expanded into the following Laurent series around $z = 0$:

$$\zeta^{(2n)}(z) = \frac{(2n)!}{z^{2n+1}} - \sum_{k=0}^{\infty} s_{n+k+1} \frac{(2n+2k+1)!}{(2k+1)!} z^{2k+1}, \quad s_k = \sum_{n,m} ' \frac{1}{P_{m,n}^{2k}}. \quad (3.5)$$

Substituting representations (3.1), (3.2) into boundary conditions (2.10), (2.11), we obtain the following equations in the polar system of the coordinates (r, θ) on the unit circle $r = 1$:

$$\begin{aligned} & \sum_{k=0}^{\infty} (A_n \sin(2n+1)\theta + B_n \cos(2n+1)\theta) = \\ & \text{Re } \Gamma \sin \theta + \text{Im } \Gamma \cos \theta + \sum_{n=0}^{\infty} (-C_n \sin(2n+1)\theta + D_n \cos(2n+1)\theta) - \end{aligned}$$

$$\begin{aligned}
& \sum_{n=0}^{\infty} \sum_{k=0}^{\infty} \operatorname{Im} \left[\Delta_{n,k} (C_k + iD_k) e^{i(2n+1)\theta} \right], \\
& \sum_{k=0}^{\infty} (2n+1) (A_n \sin(2n+1)\theta + B_n \cos(2n+1)\theta) - \\
& \kappa \left\{ \operatorname{Re} \Gamma \sin \theta + \operatorname{Im} \Gamma \cos \theta - \sum_{n=0}^{\infty} (2n+1) (-C_n \sin(2n+1)\theta + D_n \cos(2n+1)\theta) - \right. \\
& \left. \sum_{n=0}^{\infty} \sum_{k=0}^{\infty} \operatorname{Im} \left[(2n+1) \Delta_{n,k} (C_k + iD_k) e^{i(2n+1)\theta} \right] \right\} = \\
& -\gamma \sum_{n=0}^{\infty} (2n+1)^2 (A_n \sin(2n+1)\theta + B_n \cos(2n+1)\theta),
\end{aligned}$$

where $\kappa = \mu/\mu_1$, $\gamma = \mu_0/(\mu_1 a)$ and

$$\Delta_{n,k} = s_{n+k+1} \frac{(2n+2k+1)!}{(2n+1)!(2k)!}.$$

Collecting the terms associated with the functions $\sin(2n+1)\theta$ and $\cos(2n+1)\theta$, we obtain the following infinite system of linear algebraic equations:

$$A_n = \operatorname{Re} \Gamma \delta_{n,0} - C_n - \sum_{k=0}^{\infty} (C_k \operatorname{Re} \Delta_{n,k} - D_k \operatorname{Im} \Delta_{n,k}), \quad n = 0, 1, 2, \dots, \quad (3.6)$$

$$B_n = \operatorname{Im} \Gamma \delta_{n,0} + D_n - \sum_{k=0}^{\infty} (C_k \operatorname{Im} \Delta_{n,k} + D_k \operatorname{Re} \Delta_{n,k}), \quad n = 0, 1, 2, \dots, \quad (3.7)$$

$$\begin{aligned}
A_n - \kappa \operatorname{Re} \Gamma \delta_{n,0} - \kappa C_n + \kappa \sum_{k=0}^{\infty} (C_k \operatorname{Re} \Delta_{n,k} - D_k \operatorname{Im} \Delta_{n,k}) &= -\gamma(2n+1)A_n, \quad (3.8) \\
n &= 0, 1, 2, \dots,
\end{aligned}$$

$$\begin{aligned}
B_n - \kappa \operatorname{Im} \Gamma \delta_{n,0} + \kappa D_n + \kappa \sum_{k=0}^{\infty} (C_k \operatorname{Im} \Delta_{n,k} + D_k \operatorname{Re} \Delta_{n,k}) &= -\gamma(2n+1)B_n, \quad (3.9) \\
n &= 0, 1, 2, \dots,
\end{aligned}$$

where $\delta_{n,k}$ is the Kronecker delta function.

Solution of (3.6)-(3.9) for the coefficients A_n and B_n has the form

$$A_n = \frac{2\kappa C_n}{1 - \kappa + \gamma(2n+1)}, \quad B_n = -\frac{2\kappa D_n}{1 - \kappa + \gamma(2n+1)}. \quad (3.10)$$

Then we obtain the following infinite system of linear equations for the coefficients C_n , D_n :

$$\frac{1 + \kappa + \gamma(2n+1)}{1 - \kappa + \gamma(2n+1)} C_n + \sum_{k=0}^{\infty} (C_k \operatorname{Re} \Delta_{n,k} - D_k \operatorname{Im} \Delta_{n,k}) = \operatorname{Re} \Gamma \delta_{n,0}, \quad (3.11)$$

$$\frac{1 + \kappa + \gamma(2n + 1)}{1 - \kappa + \gamma(2n + 1)} D_n - \sum_{k=0}^{\infty} (C_k \operatorname{Im} \Delta_{n,k} + D_k \operatorname{Re} \Delta_{n,k}) = -\operatorname{Im} \Gamma \delta_{n,0}, \quad (3.12)$$

$$n = 0, 1, 2, \dots$$

4 Effective properties of the doubly-periodic lattices

Effective elastic moduli of a composite containing some arbitrary doubly-periodic array of inhomogeneities can be represented by the following tensor:

$$\mathbf{C}^* = \begin{bmatrix} C_{11}^* & C_{12}^* \\ C_{12}^* & C_{22}^* \end{bmatrix} \quad (4.1)$$

The relationship between the average stresses $\langle [\sigma_{xz}, \sigma_{yz}]^T \rangle$ and the average strains $\langle [\varepsilon_{xz}, \varepsilon_{yz}]^T \rangle$ are expressed via \mathbf{C}^* as

$$\langle [\sigma_{31}, \sigma_{32}]^T \rangle = \mathbf{C}^* \langle [\varepsilon_{31}, \varepsilon_{32}]^T \rangle. \quad (4.2)$$

Following [2], we express the average values of these components as follows:

$$\left\langle \begin{bmatrix} \sigma_{31} \\ \sigma_{32} \end{bmatrix} \right\rangle = \frac{\mu_1}{S} \int_{S_{int}} \begin{bmatrix} u_{3,1} \\ u_{3,2} \end{bmatrix} dS + \frac{\mu}{S} \int_{S_{ext}} \begin{bmatrix} u_{3,1} \\ u_{3,2} \end{bmatrix} dS - \frac{1}{S} \int_{\partial S_{int}} (\sigma_{r3}^1 - \sigma_{r3}) \begin{bmatrix} x \\ y \end{bmatrix} ds, \quad (4.3)$$

$$\left\langle \begin{bmatrix} \varepsilon_{31} \\ \varepsilon_{32} \end{bmatrix} \right\rangle = \frac{1}{2S} \int_{S_{int}} \begin{bmatrix} u_{3,1} \\ u_{3,2} \end{bmatrix} dS + \frac{1}{2S} \int_{S_{ext}} \begin{bmatrix} u_{3,1} \\ u_{3,2} \end{bmatrix} dS, \quad (4.4)$$

where $S = 4\omega_1 \operatorname{Im} \omega_2$ is the area of the parallelogram $A_1A_2A_3A_4$, $S_{int} = \pi a^2$ is the area of the inhomogeneity, and $S_{ext} = S \setminus S_{int}$ is the area of the period parallelogram located outside of the inhomogeneity, and dS and ds denote correspondingly integration by area and by arc length.

Using representations (3.1), (3.2), and Green's theorem, we evaluate the integrals

$$\int_{S_{int}} u_{3,1} dS = \pi a^2 B_0, \quad \int_{S_{int}} u_{3,2} dS = \pi a^2 A_0, \quad (4.5)$$

$$\int_{S_{ext}} u_{3,1} dS = 4 \operatorname{Im} (\Gamma \omega_1 + a(C_0 + iD_0)\eta_1) \operatorname{Im} \omega_2 - \pi a^2 B_0, \quad (4.6)$$

$$\int_{S_{ext}} u_{3,2} dS = -4 \operatorname{Im} (\Gamma \omega_1 + a(C_0 + iD_0)\eta_1) \operatorname{Re} \omega_2 +$$

$$4 \operatorname{Im} (\Gamma \omega_2 + a(C_0 + iD_0)\eta_2) \operatorname{Re} \omega_1 - \pi a^2 A_0. \quad (4.7)$$

For the last term in the formula (4.3), using boundary condition (2.11), we write:

$$\frac{1}{S} \int_{\partial S_{int}} (\sigma_{r3}^1 - \sigma_{r3}) \begin{bmatrix} x \\ y \end{bmatrix} ds = \frac{\mu_0}{S} \int_0^{2\pi} \frac{\partial^2}{\partial \theta^2} [\operatorname{Im} f_1(at)] \begin{bmatrix} \cos \theta \\ \sin \theta \end{bmatrix} d\theta = \quad (4.8)$$

$$-f \frac{\mu_0}{a} \begin{bmatrix} B_0 \\ A_0 \end{bmatrix},$$

where $f = \pi a^2/S$ is the volume fraction of the inhomogeneity.

To obtain the effective properties, assume first that the only nonzero loading at infinity is $\sigma_{32}^\infty/\mu = 1$. In this case, $\Gamma = 1$. Denote by the index $[1, 0]$ all the parameters corresponding to this case. In particular, $A_0^{[1,0]}$, $B_0^{[1,0]}$, $C_0^{[1,0]}$, and $D_0^{[1,0]}$ correspond to the solutions of system (3.10), (3.11), (3.12) obtained with $\Gamma = 1$. Then

$$\begin{aligned} \left\langle \begin{bmatrix} \varepsilon_{31}^{[1,0]} \\ \varepsilon_{32}^{[1,0]} \end{bmatrix} \right\rangle = \frac{2f}{\pi} & \begin{bmatrix} (C_0^{[1,0]} \operatorname{Im} \eta_1 + D_0^{[1,0]} \operatorname{Re} \eta_1) \operatorname{Im} \omega_2/a \\ -(C_0^{[1,0]} \operatorname{Im} \eta_1 + D_0^{[1,0]} \operatorname{Re} \eta_1) \operatorname{Re} \omega_2/a + \\ (\operatorname{Im} \omega_2/a + C_0^{[1,0]} \operatorname{Im} \eta_2 + D_0^{[1,0]} \operatorname{Re} \eta_2) \omega_1/a \end{bmatrix}, \end{aligned} \quad (4.9)$$

$$\begin{aligned} \left\langle \begin{bmatrix} \sigma_{31}^{[1,0]} \\ \sigma_{32}^{[1,0]} \end{bmatrix} \right\rangle = \frac{4\mu f}{\pi} & \begin{bmatrix} \pi\delta/4B_0^{[1,0]} + (C_0^{[1,0]} \operatorname{Im} \eta_1 + D_0^{[1,0]} \operatorname{Re} \eta_1) \operatorname{Im} \omega_2/a \\ \pi\delta/4A_0^{[1,0]} - (C_0^{[1,0]} \operatorname{Im} \eta_1 + D_0^{[1,0]} \operatorname{Re} \eta_1) \operatorname{Re} \omega_2/a + \\ (\operatorname{Im} \omega_2/a + C_0^{[1,0]} \operatorname{Im} \eta_2 + D_0^{[1,0]} \operatorname{Re} \eta_2) \omega_1/a \end{bmatrix}, \end{aligned} \quad (4.10)$$

where $\delta = (1 - \kappa + \gamma)/\kappa$.

Similarly, assuming $\sigma_{13}^\infty/\mu = 1$ and $\sigma_{13}^\infty/\mu = 0$, we obtain $\Gamma = i$. Denote the corresponding values with the index $[0, 1]$. Then the corresponding values of the average stresses and strains become:

$$\begin{aligned} \left\langle \begin{bmatrix} \varepsilon_{31}^{[0,1]} \\ \varepsilon_{32}^{[0,1]} \end{bmatrix} \right\rangle = \frac{2f}{\pi} & \begin{bmatrix} (\omega_1/a + C_0^{[0,1]} \operatorname{Im} \eta_1 + D_0^{[0,1]} \operatorname{Re} \eta_1) \operatorname{Im} \omega_2/a \\ -(\omega_1/a + C_0^{[0,1]} \operatorname{Im} \eta_1 + D_0^{[0,1]} \operatorname{Re} \eta_1) \operatorname{Re} \omega_2/a + \\ (\operatorname{Re} \omega_2/a + C_0^{[0,1]} \operatorname{Im} \eta_2 + D_0^{[0,1]} \operatorname{Re} \eta_2) \omega_1/a \end{bmatrix}, \end{aligned} \quad (4.11)$$

$$\begin{aligned} \left\langle \begin{bmatrix} \sigma_{31}^{[0,1]} \\ \sigma_{32}^{[0,1]} \end{bmatrix} \right\rangle = \frac{4\mu f}{\pi} & \begin{bmatrix} \pi\delta/4B_0^{[0,1]} + (\omega_1/a + C_0^{[0,1]} \operatorname{Im} \eta_1 + D_0^{[0,1]} \operatorname{Re} \eta_1) \operatorname{Im} \omega_2/a \\ \pi\delta/4A_0^{[0,1]} - (\omega_1/a + C_0^{[0,1]} \operatorname{Im} \eta_1 + D_0^{[0,1]} \operatorname{Re} \eta_1) \operatorname{Re} \omega_2/a + \\ (\operatorname{Re} \omega_2/a + C_0^{[0,1]} \operatorname{Im} \eta_2 + D_0^{[0,1]} \operatorname{Re} \eta_2) \omega_1/a \end{bmatrix}. \end{aligned} \quad (4.12)$$

Using the average values given by (4.9)-(4.12) as columns, we can create the matrices:

$$\boldsymbol{\Sigma} = \left[\left\langle \begin{bmatrix} \sigma_{31}^{[1,0]} \\ \sigma_{32}^{[1,0]} \end{bmatrix} \right\rangle, \left\langle \begin{bmatrix} \sigma_{31}^{[0,1]} \\ \sigma_{32}^{[0,1]} \end{bmatrix} \right\rangle \right], \quad (4.13)$$

$$\mathbf{E} = \left[\left\langle \begin{bmatrix} \varepsilon_{31}^{[1,0]} \\ \varepsilon_{32}^{[1,0]} \end{bmatrix} \right\rangle, \left\langle \begin{bmatrix} \varepsilon_{31}^{[0,1]} \\ \varepsilon_{32}^{[0,1]} \end{bmatrix} \right\rangle \right]. \quad (4.14)$$

The matrices \mathbf{E} and $\boldsymbol{\Sigma}$ are related by the formula (4.2) as:

$$\boldsymbol{\Sigma} = \mathbf{C}^* \mathbf{E}. \quad (4.15)$$

Correspondingly, we can obtain the following formula for the matrix of the effective properties \mathbf{C}^* :

$$\mathbf{C}^* = \boldsymbol{\Sigma} \mathbf{E}^{-1}. \quad (4.16)$$

5 Effective shear moduli of regular lattices

In the case of regular lattices (square and hexagonal), the displacements can be represented by series with real coefficients

$$u_3^1(z) = \Gamma a \sum_{n=0}^{\infty} B_n \left(\frac{z}{a} \right)^{2n+1}, \quad (5.1)$$

$$u_3(z) = \Gamma z + \Gamma a \sum_{n=0}^{\infty} \frac{a^{2n+1}}{(2n)!} D_n \zeta^{(2n)}(z). \quad (5.2)$$

For such lattices all lattice sums are real. We introduce the dimensionless parameter

$$h = \frac{a}{\ell}, \quad (5.3)$$

where $\ell = 2|\omega_1|$, and the dimensionless lattice sums

$$S_k = \sum_{n,m} \left(\frac{\ell}{P_{m,n}} \right)^{2k}, \quad k = 2, 3, \dots \quad (5.4)$$

Then compliance with the boundary conditions leads to the system of linear equations

$$B_n = \delta_{n,0} + D_n - \sum_{n,m=0}^{\infty} \Lambda_{n,m} h^{2n+2m+2} D_m, \quad (5.5)$$

$$\mu_1 B_n = \mu \left[\delta_{n,0} - D_n - \sum_{n,m=0}^{\infty} \Lambda_{n,m} h^{2n+2m+2} D_m \right] - \frac{\mu_0}{a} (2n+1) B_n, \quad (5.6)$$

where

$$\Lambda_{n,m} = S_{n+m+1} \frac{(2n+2m+1)!}{(2m)!(2n+1)!}. \quad (5.7)$$

Then for the determination of the unknown coefficients we obtain the following system

$$B_n = -\frac{2\mu}{\mu_1 - \mu + \frac{\mu_0}{a} (2n+1)} D_n, \quad (5.8)$$

$$D_n - \alpha_n \sum_{n,m=0}^{\infty} \Lambda_{n,m} h^{2n+2m+2} D_m = -\alpha_0 \delta_{n,0}, \quad (5.9)$$

where

$$\alpha_n = \frac{\mu_1 - \mu + \frac{\mu_0}{a} (2n+1)}{\mu_1 + \mu + \frac{\mu_0}{a} (2n+1)}. \quad (5.10)$$

To calculate the average strain, we evaluate the integrals

$$\int_{S_{int}} u_x \, dS = \Gamma \int_0^{2\pi} \int_0^a \sum_{n=0}^{\infty} (2n+1) B_n \left(\frac{r}{a}\right)^{2n} e^{2\pi n i} r dr d\phi = \Gamma \pi a^2 B_0. \quad (5.11)$$

$$\begin{aligned} \int_{S_{ext}} u_x \, dS &= \oint_{\partial S_{ext}} u \, dy = \oint_{\partial S} u \, dy - \oint_{r=a} u \, dy = \Gamma \left\{ \oint_{\partial S} z \, dy + a \sum_{n=0}^{\infty} \frac{a^{2n+1}}{(2n)!} D_n \times \right. \\ &\quad \left. \oint_{\partial S} \zeta^{(2n)}(z) \, dy - a \sum_{n=0}^{\infty} B_n \oint_{r=a} \cos(2n+1)\phi \, dy \right\} \\ &= \Gamma \{ S + 4a^2 B_0 \eta_1 \text{Im} \omega_2 - \pi a^2 B_0 \}, \end{aligned} \quad (5.12)$$

where the quasiperiodicity of $\zeta(z)$ and Green's theorem have been used in the calculation of contour integrals. Then the average strain is

$$\langle u_x \rangle = \frac{1}{S} \left(\int_{S_{int}} u_x \, dS + \int_{S_{ext}} u_x \, dS \right) \quad (5.13)$$

where f is the volume fraction of the inhomogeneities and $\eta_1 \text{Im} \omega_2 = \frac{\pi}{4}$ for both the square and the hexagonal lattices.

The average shear stress has the form

$$\begin{aligned}
\langle \sigma_{xz} \rangle &= \frac{1}{S} \left(\mu_1 \int_{S_{int}} u_x \, dS + \mu \int_{S_{ext}} u_x \, dS + a^2 \int_0^{2\pi} \left[\mu \frac{\partial u}{\partial r} \right] \cos \phi \, d\phi \right) \\
&= \frac{1}{S} \left(\mu_1 \int_{S_{int}} u_x \, dS + \mu \int_{S_{ext}} u_x \, dS + \Gamma \mu_0 \pi a B_0 \right) \\
&= \Gamma \left[\mu + \left(\mu_1 - \mu + \frac{\mu_0}{a} \right) f B_0 + \frac{4}{\pi} \mu f \eta_1 \operatorname{Im} \omega_2 D_0 \right] \\
&= \Gamma \left[\mu + \left(\mu_1 - \mu + \frac{\mu_0}{a} \right) f B_0 + \mu f D_0 \right] = \Gamma \mu [1 - f D_0], \tag{5.14}
\end{aligned}$$

since for both the square and the hexagonal lattices $\eta_1 \operatorname{Im} \omega_2 = \frac{\pi}{4}$.

The effective shear modulus μ_{eff} relates the average shear stress $\langle \sigma_{xz} \rangle$ and the average strain $\langle u_x \rangle$ as

$$\langle \sigma_{xz} \rangle = \mu_{\text{eff}} \langle u_x \rangle, \tag{5.15}$$

and therefore equals

$$\mu_{\text{eff}} = \mu \frac{1 - f D_0}{1 + f D_0}. \tag{5.16}$$

If the volume fraction of the inhomogeneities is small, $f \ll 1$, then $D_0 \approx -\alpha_0$. In this case, (5.16) gives the following approximation

$$\mu_{\text{eff}} = \mu \frac{1 + f \alpha_0}{1 - f \alpha_0}, \tag{5.17}$$

where

$$\alpha_0 = \frac{\mu_1 - \mu + \frac{\mu_0}{a}}{\mu_1 + \mu + \frac{\mu_0}{a}}. \tag{5.18}$$

Below we analyze effective shear moduli of specific lattices.

5.1 Square lattice

Solution of (5.9) can also be obtained as a convergent power series in terms of the parameter $h = \frac{a}{\ell} < \frac{1}{2}$, where $\ell = |2\omega_1| = |2\omega_2|$. The only nonzero sums S_k in (5.4), (5.7), and (5.9) are those with $k = 2n, n = 1, 2, \dots$. Then the series expansion of D_0 for the square lattice has the form

$$D_0 = -\alpha_0 - 3\alpha_0^2 \alpha_1 S_2^2 h^8 - (9\alpha_0^3 \alpha_1^2 S_2^4 + 7\alpha_0^2 \alpha_3 S_4^2) h^{16} + O(h^{24}), \tag{5.19}$$

where S_2, S_4 are normalized lattice sum

$$S_2 = \sum'_{m,n} \frac{1}{(n+im)^4} \approx 3.15121, \quad (5.20)$$

$$S_4 = \sum'_{m,n} \frac{1}{(n+im)^8} \approx 4.25577. \quad (5.21)$$

The series expansion of D_0 (5.19) provides a good approximation of the effective shear modulus even for the high volume fraction of the inhomogeneities as shown in Figure 2.

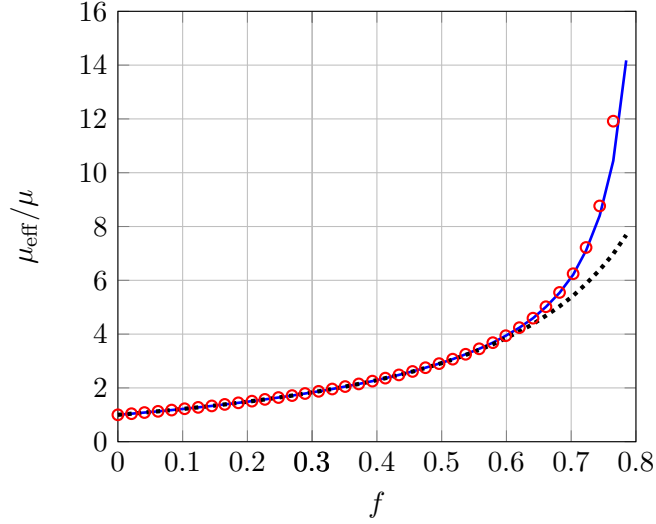


Figure 2: Dependence of the normalized shear modulus for a square lattice of cylindrical inhomogeneities with $\mu_1/\mu = 100$ and $\gamma = 9905$ on the inhomogeneities' volume fraction f . The red circles correspond to exact numerical calculations by (5.16), the blue solid line depicts approximation (5.19) in (5.16), while the black dotted line refers to the dilute approximation (5.17).

5.2 Hexagonal lattice

The only nonzero sums for the hexagonal lattice are $S_{3n}, n = 1, 2, \dots$. The series expansion of D_0 in (5.9) has the form

$$D_0 = -\alpha_0 - 5\alpha_0^2\alpha_2 S_3^2 h^{12} - \alpha_0^2 (25\alpha_0\alpha_2 S_3^4 + 11\alpha_5 S_6^2) h^{24} + O(h^{32}), \quad (5.22)$$

where the values of normalized lattice sums S_3, S_6 are

$$S_3 = \sum'_{m,n} \frac{1}{\left(n + me^{\frac{\pi i}{3}}\right)^6} \approx 5.86303, \quad (5.23)$$

$$S_6 = \sum'_{m,n} \frac{1}{\left(n + me^{\frac{\pi i}{3}}\right)^{12}} \approx 6.00964. \quad (5.24)$$

The series expansion of D_0 (5.22) provides an excellent approximation of the effective shear modulus even for the high volume fraction of the inhomogeneities as shown in Figure 3.

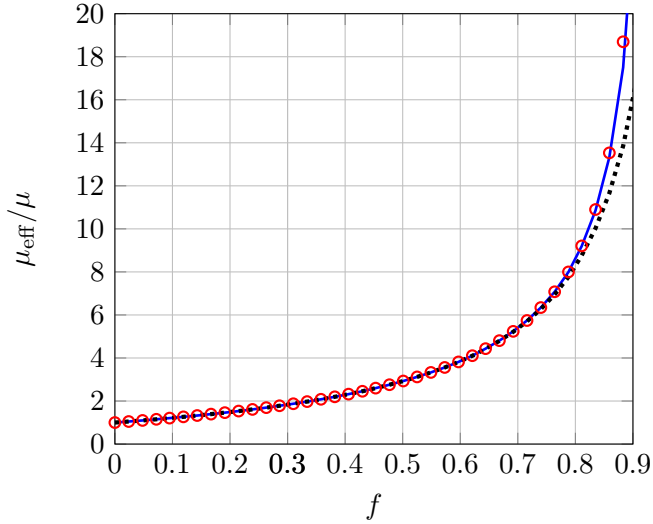


Figure 3: Dependence of the normalized shear modulus for a hexagonal lattice of cylindrical inhomogeneities with $\mu_1/\mu = 100$ and $\gamma = 9905$ on the inhomogeneities' volume fraction f . The red circles correspond to exact numerical calculations by (5.16), the blue solid line depicts approximation (5.22) in (5.16), while the black dotted line refers to the dilute approximation (5.17).

6 Numerical results

6.1 Evaluation of the local fields and the effective properties: Example 1

In this example, we demonstrate that the proposed approach allows for the accurate evaluation of the local fields as well as for the overall properties of the composite. We choose the following material parameters: $\kappa = 100$, $\gamma = 9905$ and take the unit cell to be of a general parallelogram shape with $\text{Im } \omega_2/\omega_1 = 1$ and with the smaller angle of the parallelogram $\beta = 5\pi/12$. The volume fraction of the inhomogeneity in the cell

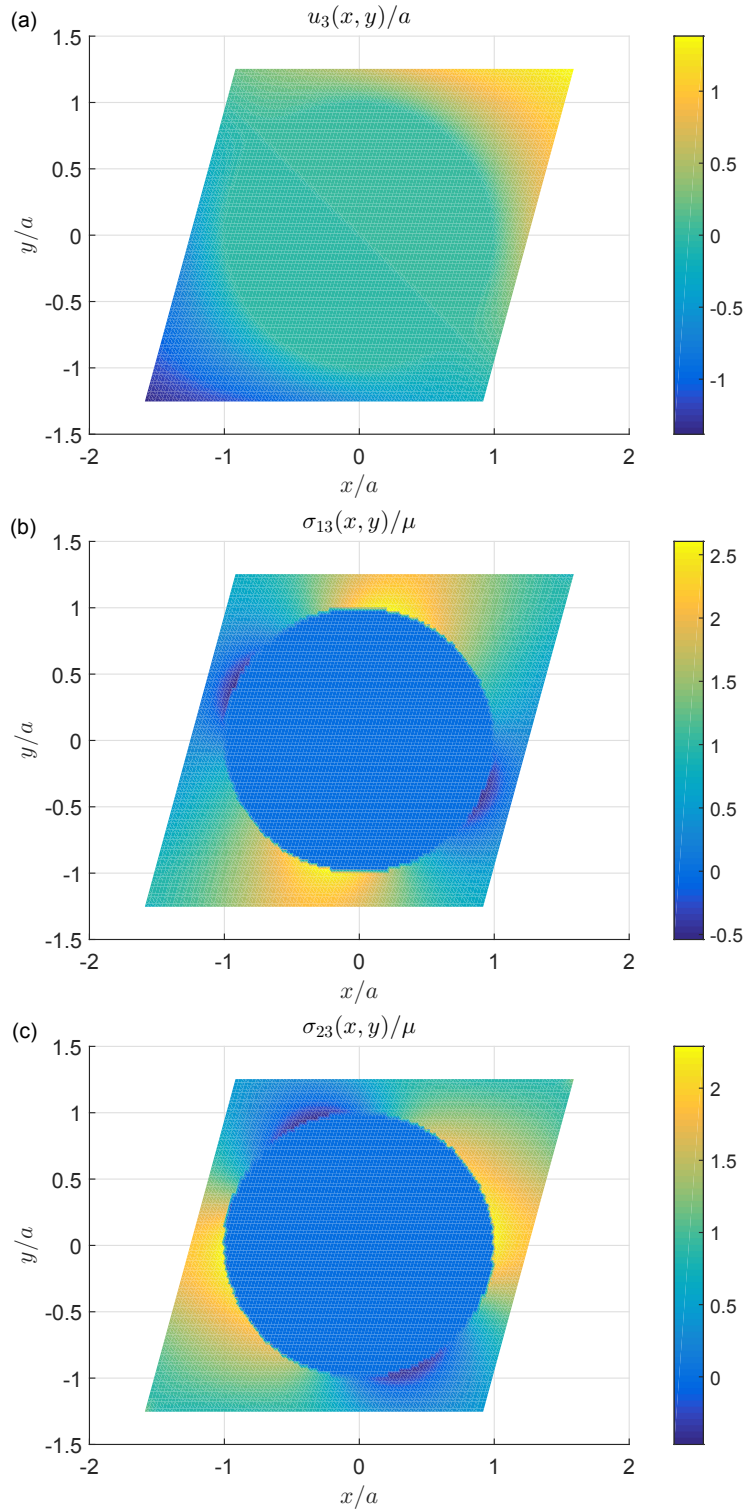


Figure 4: Distributions of the dimensionless displacements and stresses inside the general parallelogram unit cell with $\text{Im } \omega_2/\omega_1 = 1$, and $\beta = 5\pi/12$.

	Hexagonal array, $f = 0.8$	Square array, $f = 0.7$	Rectangular array, $ \omega_2 /\omega_1 = 0.5$, $f = 0.36$	General doubly-periodic array, $ \omega_2 /\omega_1 = 0.5$, $\beta = \pi/3$, $f = 0.48$			
	$\frac{C_{11}^*}{2\mu} = \frac{C_{22}^*}{2\mu}$	$\frac{C_{11}^*}{2\mu} = \frac{C_{22}^*}{2\mu}$	$\frac{C_{11}^*}{2\mu}$	$\frac{C_{22}^*}{2\mu}$	$\frac{C_{11}^*}{2\mu}$	$\frac{C_{22}^*}{2\mu}$	$\frac{C_{12}^*}{2\mu}$
Our results	8.2603	6.3359	1.8840	4.1978	2.9692	4.4972	1.3256
Yan et al. [30]	8.2600	6.3359	1.6899	4.1978	2.9600	4.4977	1.3248

Table 1: Comparison of our results with the estimates by Yan et al. [30] for composites with perfectly bonded inhomogeneities.

is taken to be $f = 0.5$ and the loading Γ at infinity is given by $\Gamma = 1 + 1i$. Using Eqs. (2.4)-(2.5), the displacement $u_3(x, y)$ and the stress components $\sigma_{13}(x, y)$, $\sigma_{23}(x, y)$ have been computed; the contours of their normalized values are presented in Figs. 4. It is seen from Fig. 4a that the displacement $u_3(x, y)/a$ is indeed continuous everywhere in the cell. Also, the displacement is skew-symmetric with respect to the origin, as expected for the loading conditions enforced at infinity. Figs. 4b,c illustrate the distributions of the dimensionless stress components $\sigma_{13}(x, y)/\mu$ and $\sigma_{23}(x, y)/\mu$. As expected, $\sigma_{13}(x, y)/\mu$ and $\sigma_{23}(x, y)/\mu$ are discontinuous across the interface and that the distributions of $\sigma_{13}(x, y)/\mu$ and $\sigma_{23}(x, y)/\mu$ are symmetric with respect to the origin. From the analysis of these figures, one can conclude that the developed solution works well even for the composites with relatively high volume fractions of the inhomogeneities. The effective properties for the composite considered in this example have been evaluated using equations of Section 4. They are $C_{11}^*/(2\mu) = 3.0750$, $C_{12}^*/(2\mu) = 0.0863$, $C_{22}^*/(2\mu) = 2.8697$.

6.2 Comparison with the existing results for the effective properties

In this section, we compare the effective properties estimates obtained with the present approach with those reported in the literature.

We start with the case of perfectly bonded inhomogeneities, which is characterized by the parameter $\mu_0 = 0$. This case has been previously investigated by many authors and several numerical results are available. Such solutions are presented in [30] where they are compared with two previous estimates. We choose the shear moduli of the inhomogeneity and the matrix such that the parameter κ is equal to $\kappa = 0.02$ and evaluate the effective properties of the composites characterized by various shapes of unit cells and various volume fractions of inhomogeneities. The angle β corresponds to the smallest angle of the parallelogram period cell. In table 1, we compare our estimates with those reported in [30].

The table shows that our results have excellent agreement with the estimates in [30] in most of the cases considered. The only estimate that does not perfectly agree with ours is that for $C_{11}^*/2\mu$ and the rectangular array. This result was compared in

	Hexagonal array, $f = 0.8$	Square array, $f = 0.7$	Rhombic array, $f = 0.7, \omega_1 = 1, \omega_2 = 0.5 + 1i$	General doubly-periodic array, $\text{Im } \omega_2/\omega_7 = 0.5, \beta = 5\pi/12, f = 0.7$			
	$\frac{C_{11}^*}{2\mu} = \frac{C_{22}^*}{2\mu}$	$\frac{C_{11}^*}{2\mu} = \frac{C_{22}^*}{2\mu}$	$\frac{C_{11}^*}{2\mu}$	$\frac{C_{22}^*}{2\mu}$	$\frac{C_{11}^*}{2\mu}$	$\frac{C_{22}^*}{2\mu}$	$\frac{C_{12}^*}{2\mu}$
Our results	9.0532	6.8758	7.3080	4.7771	7.1407	5.5385	0.4449
Yan et al [30]	8.9926	6.8380	7.2652	4.7618	7.0997	5.5160	0.4401

Table 2: Comparison of our results with the estimates by Yan et al., [30] for coated inhomogeneities.

[30] with only one estimate that was obtained previously by some authors of the latter paper, so the reason for the disagreement with our result is not clear. To perform another check of our results, we recomputed them using the expressions in [27] for unit cells of the same shapes. Here agreement was perfect for all cases considered and, for this reason, the results are not presented here.

The paper [30] also contains estimates for the composites with highly conducting coating layers. The authors adopted the following parameters (in our notations): $\kappa = 100$, $\mu_c/\mu = 990.5$, $h_l/H = 0.1$. Those parameters satisfy condition (2.10), which allows for the comparison of estimates [30] for composites with coated inhomogeneities with those obtained by the proposed approach for composites with superconducting interfaces. To do that we use Eq. (2.11) to evaluate the value of the parameter $\gamma = \mu_c h_l / H \mu_1$ to be $\gamma = 9905$. The comparison of our results with those reported in [30] is presented in table 2. As expected, the results do not match exactly, especially for anisotropic configurations. However, the agreement is quite good, provided that the two different interface models are used. Note, that the example presented in [30] for a rhombic array with the volume fraction $f = 0.7$ is not realistic, as the inhomogeneity in such a case cannot be fitted inside the unit cell.

Finally, to illustrate the importance of accurate accounting for geometrical arrangement of the inhomogeneities in the unit cell, in Fig. 5 we compare our results with the dilute estimates of [2] and the Mori-Tanaka estimates of [7]. The square lattice is chosen for the arrangement of the inhomogeneities and the parameters for the matrix, inhomogeneity, and interface are taken to be the same as in the sample used in table 2. As expected, dilute estimates work well only for the composites with low volume fractions of inhomogeneities. The Mori-Tanaka-based estimates perform better but still under-predict the effective properties in case of high volume fractions.

To study the influence of the unit cell shape, on Fig. 6 we plotted the effective properties of composites with unit cells of various shapes as functions of the volume fraction f . The values $\kappa = 100$ and $\gamma = 9905$ were selected for the material parameters. For the square and hexagonal lattices, the graphs of $C_{11}^*/(2\mu) = C_{22}^*/(2\mu)$ are plotted. For the rhombic and general doubly-periodic arrays, two graphs of $C_{11}^*/(2\mu)$ and $C_{22}^*/(2\mu)$ are plotted. The values of $C_{12}^*/(2\mu)$ in all cases are either equal to zero

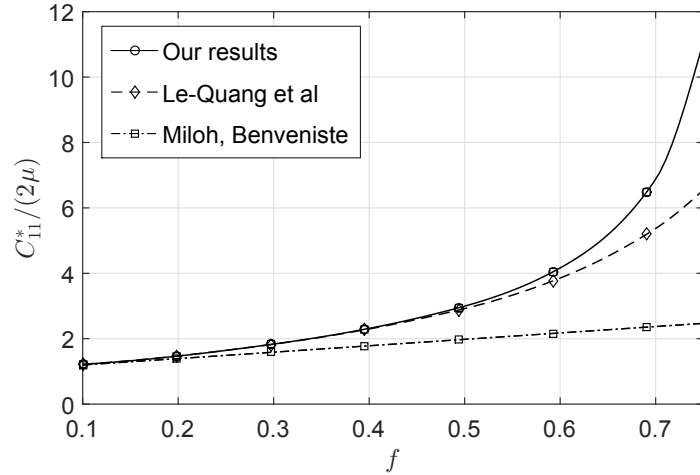


Figure 5: Comparison with the estimates of Quang et al [7] and Miloh & Benveniste [2] for $\kappa = 100$ and $\gamma = 9905$.

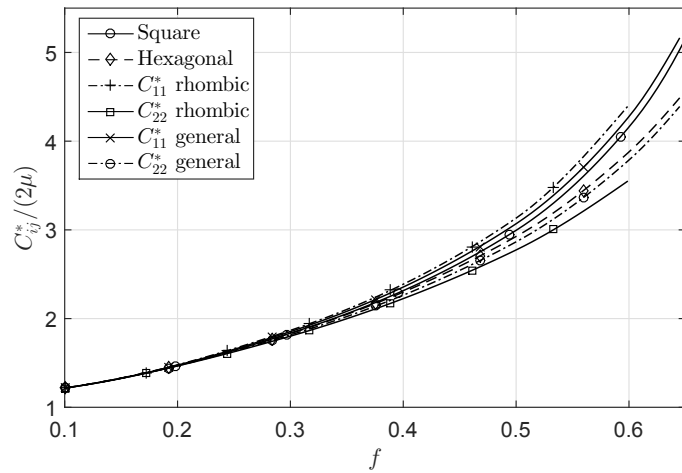


Figure 6: Effective properties vs. volume fraction f for composites with various unit cells for $\kappa = 100$ and $\gamma = 9905$.

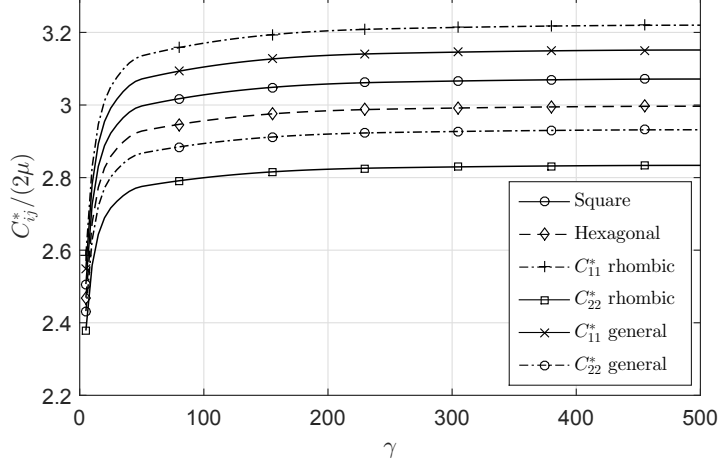


Figure 7: Effective properties vs. parameter γ for composites with various unit cells and $\kappa = 0.5$.

or relatively small compared to those for $C_{11}^*/(2\mu)$ and $C_{22}^*/(2\mu)$; they are not shown in Fig. 6. It can be concluded that the influence of the unit cell shape increases with the increase in the volume fraction of inhomogeneities.

To illustrate the influence of the interface parameter γ , in Fig. 7 we plotted the effective properties of composites with various lattices of inhomogeneities as functions of parameter γ . The value of the parameter κ is chosen to be $\kappa = 0.5$. For the square and hexagonal lattices the graphs of $C_{12}^*/(2\mu) = C_{11}^*/(2\mu) = C_{22}^*/(2\mu)$ are plotted. For the rhombic and general doubly-periodic arrays, two graphs of $C_{11}^*/(2\mu)$ and $C_{22}^*/(2\mu)$ are plotted. As before, the values of $C_{12}^*/(2\mu)$ in all cases are either equal to zero or relatively small compared to $C_{11}^*/(2\mu)$ and $C_{22}^*/(2\mu)$ and are not shown in Fig. 7. It can be concluded that initial increase in γ triggers rapid increase in the values of $C_{12}^*/(2\mu)$, which are different for different unit cells. However, after reaching some plato (also different for each case of a unit cell), those values vary just slightly.

7 Conclusion

In this paper, we developed an analytical solution for modeling harmonics problems involving two-dimensional composites with a homogeneous matrix and arbitrary doubly periodic arrays of identical circular inhomogeneities with superconducting or membrane-type interfaces. The solution allows for the accurate evaluation of the local fields everywhere in the composite system and for its overall properties. For the composites with square and hexagonal arrangements of inhomogeneities, explicit formulas are provided to most effectively determine their overall properties. Comparisons with the existing numerical solutions are performed and a set of reliable benchmark results is established. The developed analytical solution can be used in

wide areas of applications particularly those related to modeling modern materials with improved thermal, electrical, and mechanical properties.

Acknowledgment

The work of the first author (A.Z.) was supported by Simons Foundation through the Simons Collaboration Grant for Mathematicians (2020-2025), award number 713080. This support is gratefully acknowledged here. The third author (S.M.) gratefully acknowledges the support from the National Science Foundation, award number NSF CMMI - 2112894 and from the Theodore W. Bennett Chair, University of Minnesota.

Appendix A Properties of the system of Eqs. (3.11), (3.12)

The system of Eqs. (3.11), (3.12) can be written as

$$\mathbf{x}_n - \sum_{k=0}^{\infty} \mathbf{G}_{nk} \mathbf{x}_k = \mathbf{y}_0 \delta_{n,0}, \quad n = 0, 1, 2, \dots, \quad (\text{A.1})$$

where

$$\begin{aligned} \mathbf{x}_n &= \begin{bmatrix} C_n \\ D_n \end{bmatrix}, \quad \mathbf{G}_{nk} = \alpha_n \begin{bmatrix} -\text{Re } \Delta_{nk} & \text{Im } \Delta_{nk} \\ \text{Im } \Delta_{nk} & \text{Re } \Delta_{nk} \end{bmatrix}, \quad \mathbf{y}_0 = \alpha_0 \begin{bmatrix} \text{Re } \Gamma \\ \text{Im } \Gamma \end{bmatrix}, \\ \mathbf{G}_{00} &= \mathbf{0}, \\ \alpha_n &= \frac{1 - \kappa + \gamma(2n + 1)}{1 + \kappa + \gamma(2n + 1)} \end{aligned}$$

Introduce an operator on the vector space $l^\infty(\mathbb{R}^2)$ of bounded sequences whose elements are two-dimensional vectors:

$$\mathbf{x} = \{\mathbf{x}_n\}_{n=0}^{\infty} = [\mathbf{x}_0, \mathbf{x}_1, \dots, \mathbf{x}_n, \dots]^T,$$

where $\mathbf{x}_n = [x_n^{(1)}, x_n^{(2)}]$. Take the norm on this space as:

$$\|\mathbf{x}\| = \sup_{n=0,1,2,\dots} \max \left\{ |x_n^{(1)}|, |x_n^{(2)}| \right\}.$$

Introduce a linear operator $\mathcal{L} : l^\infty(\mathbb{R}^2) \rightarrow l^\infty(\mathbb{R}^2)$ by the formula:

$$(\mathcal{L}\mathbf{x})_n = \sum_{k=0}^{\infty} \mathbf{G}_{nk} \mathbf{x}_k, \quad n = 0, 1, 2, \dots \quad (\text{A.2})$$

Then Eq. A.1 can be written in the operator form

$$\mathbf{x} - \mathcal{L}\mathbf{x} = \mathbf{y}, \quad (\text{A.3})$$

where $\mathbf{y}_n = \mathbf{y}_0 \delta_{n,0}$.

Theorem 1. *The operator $\mathcal{L} : l^\infty(\mathbb{R}^2) \rightarrow l^\infty(\mathbb{R}^2)$, given by the formula (A.2), is a bounded linear operator for all $a < \min\{|\omega_1|, |\omega_2|\}$*

Proof. Compute the norm of the operator \mathcal{L} .

$$\begin{aligned} \|\mathcal{L}\| &= \sup_{\|x\|=1} \|\mathcal{L}x\| = \sup_{\|x\|=1} \sup_n \left\| \sum_{k=0}^{\infty} \mathbf{G}_{nk} x_k \right\| \leq \sup_n \sum_{k=0}^{\infty} \|\mathbf{G}_{nk}\| \leq \\ &\leq \sup_n \sum_{k=0}^{\infty} |\alpha_n| (|\operatorname{Re} \Delta_{nk}| + |\operatorname{Im} \Delta_{nk}|). \end{aligned}$$

Observe first, that $\{\alpha_n\}$ is a convergent sequence, and hence, bounded, $|\alpha_n| < \alpha$. It is known [31] that

$$|s_k| < \frac{C}{\lambda_1^{2k} 2^{2k}},$$

where $\lambda_1 = \min(|\omega_1|/a, |\omega_2|/a) > 1$ and C is a constant. Also, from the properties of the binomial coefficients,

$$\frac{(2n+2k+1)!}{(2n+1)!(2k)!} < 2^{2n+2k+1}.$$

From here we obtain:

$$\|\mathcal{L}\| \leq \frac{C\alpha}{\lambda_1^{2n}(\lambda_1^2 - 1)}, \quad (\text{A.4})$$

and hence the operator \mathcal{L} is bounded.

Additionally, observe that if the sequence $\{x_n\}$ is bounded, $\|x_n\| \leq B$, then the sequence $\{\sum_{k=0}^{\infty} \mathbf{G}_{nk} x_k\}$ is a sequence convergent to $\mathbf{0}$. Using the same estimates as before,

$$\begin{aligned} \left\| \sum_{k=0}^{\infty} \mathbf{G}_{nk} x_k \right\| &\leq B \sum_{k=0}^{\infty} \|\mathbf{G}_{nk}\| \leq \\ B \sum_{k=0}^{\infty} |\alpha_n| (|\operatorname{Re} \Delta_{nk}| + |\operatorname{Im} \Delta_{nk}|) &\leq \frac{BC|\alpha|}{\lambda_1^{2n}(\lambda_1^2 - 1)}. \end{aligned}$$

□

From the estimate (A.4) follows that for λ_1 large enough, the norm of the operator \mathcal{L} is less than 1, $\|\mathcal{L}\| < 1$. Consequently, in this case, the solution to the infinite system of linear equations (3.11), (3.12) exists and is unique by the fixed point theorem.

Moreover, it can be shown that for any $\lambda_1 > 1$ the operator \mathcal{L} is compact [27]. Then the existence of the solution to this system is reducible to the existence of the solution of a certain finite system of linear algebraic equations.

References

- [1] Huy HP, Sanchez-Palencia E. 1974 Phénomènes de transmission à travers des couches minces de conductivité élevée. *Journal of Mathematical Analysis and Applications* **47**, 284–309.
- [2] Miloh T, Benveniste Y. 1999 On the effective conductivity of composites with ellipsoidal inhomogeneities and highly conducting interfaces. *Proceedings of the Royal Society of London. Series A: Mathematical, Physical and Engineering Sciences* **455**, 2687–2706.
- [3] Cheng H, Torquato S. 1997 Effective conductivity of dispersions of spheres with a superconducting interface. *Proceedings of the Royal Society of London. Series A: Mathematical, Physical and Engineering Sciences* **453**, 1331–1344.
- [4] Bonfoh N, Sabar H. 2018 Anisotropic thermal conductivity of composites with ellipsoidal inclusions and highly conducting interfaces. *International Journal of Heat and Mass Transfer* **118**, 498–509.
- [5] Gao M, Yang B, Huang Y, Wang G. 2021 Effects of general imperfect interface/interphase on the in-plane conductivity of thermal composites. *International Journal of Heat and Mass Transfer* **172**.
- [6] Le Quang H. 2016 Determination of the effective conductivity of composites with spherical and spheroidal anisotropic particles and imperfect interfaces. *International Journal of Heat and Mass Transfer* **95**, 162–183.
- [7] Le-Quang H, Bonnet G, He QC. 2010 Size-dependent Eshelby tensor fields and effective conductivity of composites made of anisotropic phases with highly conducting imperfect interfaces. *Physical Review B* **81**.
- [8] Le Quang H, Pham DC, Bonnet G, He QC. 2013 Estimations of the effective conductivity of anisotropic multiphase composites with imperfect interfaces. *International Journal of Heat and Mass Transfer* **58**, 175–187.
- [9] Lipton R, Talbot D. 2001 Bounds for the effective conductivity of a composite with an imperfect interface. *Proceedings of the Royal Society A – Mathematical, Physical and Engineering Sciences* **457**, 1501–1517.
- [10] Le Quang H, Phan TL, Bonnet G. 2011 Effective thermal conductivity of periodic composites with highly conducting imperfect interfaces. *I* **50**, 1428–1444.
- [11] Mishuris G, Oechsner A, Kuhn G. 2006 FEM-analysis of nonclassical transmission conditions between elastic structures. Part 2: Stiff imperfect interface. *CMC-Computers Materials & Continua* **4**, 137–151.
- [12] Wang BR, Liu JT, Gu ST, He QC. 2015 Numerical evaluation of the effective conductivities of composites with interfacial weak and strong discontinuities. *International Journal of Thermal Sciences* **93**, 1–20.

- [13] Yvonnet J, He QC, Toulemonde C. 2008 Numerical modelling of the effective conductivities of composites with arbitrarily shaped inclusions and highly conducting interface. *Composites Science and Technology* **68**, 2818–2825.
- [14] Benveniste Y, Miloh T. 2001 Imperfect soft and stiff interfaces in two-dimensional elasticity. *Mechanics of Materials* **33**, 309–323.
- [15] Gurtin M, Murdoch A. 1975 Continuum theory of elastic-material surfaces. *Archive for rational mechanics and analysis* **57**, 291–323.
- [16] Gurtin M, Murdoch A. 1978 Surface stress in solids. *International Journal of Solids and Structures* **14**, 431–440.
- [17] Benveniste Y. 2014 Exact results for the local fields and the effective moduli of fibrous composites with thickly coated fibers. *Journal of the Mechanics and Physics of Solids* **71**, 219–238.
- [18] Duan HL, Karihaloo BL. 2007 Thermo-elastic, properties of heterogeneous materials with imperfect interfaces: Generalized Levin’s formula and Hill’s connections. *Journal of the Mechanics and Physics of Solids* **55**, 1036–1052.
- [19] Mogilevskaya SG, Crouch SL, Stolarski HK. 2008 Multiple interacting circular nano-inhomogeneities with surface/interface effects. *Journal of the Mechanics and Physics of Solids* **56**, 2298–2327.
- [20] Baranova S, Mogilevskaya SG, Mantic V, Jimenez-Alfaro S. 2020 Analysis of the antiplane problem with an embedded zero thickness layer described by the Gurtin-Murdoch model. *Journal of Elasticity* **140**, 171–195.
- [21] Mogilevskaya SG, Zemlyanova AY, Kushch VI. 2021 Fiber- and Particle-Reinforced Composite Materials With the Gurtin-Murdoch and Steigmann-Ogden Surface Energy Endowed Interfaces. *Applied Mechanics Reviews* **73**, 050801.
- [22] Han Z, Mogilevskaya SG, Liang Y, Cheng C, Niu Z. 2021 Numerical study of the Gurtin-Murdoch model for curved interfaces: benchmark solutions and analysis of curvature-related effects. *Journal of Mechanics of Materials and Structures* **16**, 23–48.
- [23] Castro LP, Kapanadze D, Pesetskaya E. 2015 Effective conductivity of a composite material with stiff imperfect contact conditions. *Mathematical Methods in the Applied Sciences* **38**, 4638–4649.
- [24] Kapanadze D, Mishuris G, Pesetskaya E. 2015 Improved algorithm for analytical solution of the heat conduction problem in doubly periodic 2D composite materials. *Complex Variables and Elliptic Equations* **60**, 1–23.
- [25] Castro LP, Pesetskaya E. 2019 A composite material with inextensible-membrane-type interface. *Mathematics and Mechanics of Solids* **24**, 499–510.

- [26] Kuo HY. 2013 Effective property of multiferroic fibrous composites with imperfect interfaces. *Smart Materials and Structures* **22**.
- [27] Godin YA. 2012 The effective conductivity of a periodic lattice of circular inclusions. *J. Math. Phys.* **53**, 063703, 15.
- [28] Slaughter WS. 2012 *The linearized theory of elasticity*. Springer Science & Business Media.
- [29] Abramowitz M, Stegun IA, editors. 1964 *Handbook of Mathematical Functions with Formulas, Graphs, and Mathematical Tables*. Number 55 in National Bureau of Standards Applied Mathematics Series. U.S. Government Printing Office, Washington, D.C. Corrections appeared in later printings up to the 10th Printing, December, 1972. Reproductions by other publishers, in whole or in part, have been available since 1965.
- [30] Yan P, Dong JS, Chen FL, Song F. 2017 Unified complex variable solution for the effective transport properties of composites with a doubly-periodic array of fibers. *ZAMM-Zeitschrift fur Angewandte Mathematik und Mechanik* **97**, 397–413.
- [31] Grigolyuk EI, Filshtinsky LA. 1992 *Periodic piecewise homogeneous elastic structures*. Nauka, Moscow. (in Russian).
- [32] Godin YA. 2013 Effective complex permittivity tensor of a periodic array of cylinders. *J. Math. Phys.* **54**, 053505, 9.
- [33] Kantorovich LV, Krylov VI. 2018 *Approximate methods of higher analysis*. Dover Publications. Translated from the 3rd Russian edition by C. D. Benster.